JOURNAL OF GEOPHYSICAL RESEARCH, VOL. 115, A06202, doi:10.1029/2009JA014995, 2010

Click Here for Full Article

Multiscale auroral emission statistics as evidence of turbulent reconnection in Earth's midtail plasma sheet

Alex Klimas,[1] Vadim Uritsky,[2] and Eric Donovan[2]

Received 15 October 2009; revised 2 December 2009; accepted 30 December 2009; published 8 June 2010.

[1] We provide indirect evidence for turbulent reconnection in Earth's midtail plasma sheet by reexamining the statistical properties of bright, nightside auroral emission events as observed by the UVI experiment on the Polar spacecraft and discussed previously by Uritsky et al. (2002, 2003, 2006). The events are divided into two groups: (1) those that map to $|X_{\mathrm{GSM}}| < 12\ R_E$ in the magnetotail and do not show scale-free statistics and (2) those that map to $|X_{\mathrm{GSM}}| > 12\ R_E$ and do show scale-free statistics. The $|X_{\mathrm{GSM}}|$ dependence is shown to most effectively organize the events into these two groups. Power law exponents obtained for group 2 are shown to validate the conclusions of Uritsky et al. concerning the existence of critical dynamics in the auroral emissions. It is suggested that the auroral dynamics is a reflection of a critical state in the magnetotail that is based on the dynamics of turbulent reconnection in the midtail plasma sheet.

Citation: Klimas, A., V. Uritsky, and E. Donovan (2010), Multiscale auroral emission statistics as evidence of turbulent reconnection in Earth's midtail plasma sheet, *J. Geophys. Res.*, *115*, A06202, doi:10.1029/2009JA014995.

1. Introduction

[2] It has been shown that the tail's central plasma sheet resides in a far-from-equilibrium turbulent state exhibiting stochastic properties over a broad range of spatial and temporal scales [*Borovsky et al.*, 1997; *Angelopoulos et al.*, 1999; *Borovsky and Funsten*, 2003; *Vörös et al.*, 2003; *Weygand et al.*, 2003; *Volwerk et al.*, 2004; *Vörös et al.*, 2004a, 2004b, 2005; *Weygand et al.*, 2005; *Vörös et al.*, 2006; *Weygand et al.*, 2006; *Vörös et al.*, 2007]. These observations suggest that turbulence is a primary physical process in the plasma sheet, likely generated by localized magnetic reconnection and its associated fast flows and possibly playing a role in initiating reconnection by generating strong inhomogeneities in the plasma.

[3] An important clue in the search for the origin of this turbulence is that it is strongly intermittent and so its explanation requires a nonclassical approach involving localized dissipation, transient regimes, and bidirectional energy cascades. In one promising attempt in this direction, tail intermittency has been ascribed to self-organized criticality (SOC), a multiscale stochastic process producing scale-free dissipation regions that may be centers of turbulent magnetic energy conversion. In this context, the SOC hypothesis assumes that the breakdown required for intermittency of the turbulence homogeneity condition is due to propagating avalanches of plasma instabilities residing at kinetic scales [*Klimas et al.*, 2004].

[4] Our present paper provides a summary of observational evidence for SOC in the magnetotail, and it presents new statistical results, based on the mapping of auroral emission events onto the tail plasma sheet, that unambiguously relate SOC with the dynamics of the midtail region where reconnection is observed and not to the dynamics of the inner plasma sheet.

1.1. Signatures of SOC in Earth's Magnetotail

[5] In a seminal paper, *Chang* [1992] has suggested that the global coherence of Earth's magnetotail [*Baker et al.*, 1999] is a consequence of the tail residing near a forced and/or self-organized critical state. Subsequently, *Chang* [1998a, 1998b, 1999], *Chang and Wu* [2002], *Chang et al.* [2003, 2004], and, in a related simulation study, *Wu and Chang* [2000a, 2000b, 2001] have related this critical state to sporadic localized reconnections and intermittent turbulence in the tail plasma sheet.

[6] Using data obtained in the plasma sheet by the low-energy plasma instrument on the GEOTAIL spacecraft, *Angelopoulos et al.* [1999] have shown that the distribution of continuous-flow burst durations greater than 400 km/s is a power law, consistent with SOC in the plasma sheet. They have also found that the criteria established by *Lu* [1995] for a continuum system to attain the SOC state are satisfied in the magnetosphere. Angelopoulos et al. have further shown that probability distributions of flows in the plasma sheet as well as a distribution of velocity differences at spatially separated positions can be well approximated by lognormal distributions, consistent with intermittent turbulence. They argued that these statistics are indicative of eddy turbulence driven by the localized fast flows in the plasma sheet acting

[1]NASA Goddard Space Flight Center, Greenbelt, Maryland, USA.
[2]Department of Physics and Astronomy, University of Calgary, Calgary, Alberta, Canada.

Copyright 2010 by the American Geophysical Union.
0148-0227/10/2009JA014995

as jets in a fluid, in agreement with the conclusions of *Borovsky et al.* [1997] and *Borovsky and Funsten* [2003]. Furthermore, they suggested that the fast flows and driven turbulence could provide the link by which localized reconnection sites communicate with each other to provide the cross-scale coupling inherent in SOC systems. Many of the scaling properties of the turbulence and its direct relationship to the localized fast flows as envisioned by Angelopoulos et al. and Borovsky and Fundsten have been well established [*Lui*, 2001, 2002; *Vörös et al.*, 2003, 2004b, 2007; *Volwerk et al.*, 2004; *Weygand et al.*, 2005, 2006]. The relationship of this turbulence to a self-organized critical state in the magnetotail has been further suggested by *Consolini* [1997], *Uritsky and Pudovkin* [1998], and *Consolini and Chang* [2001, 2002].

[7] While time series analysis techniques invoked in the in situ studies of tail turbulence can provide important scaling constraints on its underlying mechanisms, a more direct verification of SOC requires *spatiotemporal* analysis of dissipation events similar to the analysis of energy avalanches in numerical sandpile models [*Bak et al.*, 1988]. Spatiotemporal observations are rare in space physics, with auroral imaging being a fortunate exception. Sequences of auroral images provide the opportunity to study possible avalanche scaling associated with growth and evolution of localized regions of dissipation in the tail.

[8] Adapting a method introduced by *Lui et al.* [2000], *Uritsky et al.* [2002, 2003, 2006] have examined the spatiotemporal evolution of bright nightside auroral UV emissions as detected by the Ultraviolet Imager (UVI) experiment on the Polar spacecraft during January and February of 1997 and 1998. Emission regions were identified by setting an intensity threshold and finding contiguous image pixels above this threshold. Emission events were defined as emission regions that overlapped in two or more sequential UVI images. Emission events in the region defined by 20 h $\leq$ LT $\leq$ 4 h and apex latitude $\geq$ 55° were included. Methods were applied that are normally used for examining numerical avalanching models of SOC [*Bak et al.*, 1987, 1988; *Jensen*, 1998]. It was found [*Uritsky and Klimas*, 2004] that in many important respects the dynamics of the auroral emission events parallels that of avalanches in the directed-sandpile class of SOC models [*Hughes and Paczuski*, 2002]. Energy, size, and duration probability distributions; growth and survival dynamic distributions; relationships between energy, size, and duration; and fractal properties such as roughness, growth, and boundary dimensions were shown to exhibit power law forms over significant ranges. Moreover, the defining power law exponents were shown to be interrelated, satisfying scaling relations [*Paczuski et al.*, 1996; *Jensen*, 1998; *Munoz et al.*, 1999] that must be satisfied for systems in SOC. The strength of the relationship uncovered by Uritsky et al. between the dynamics of the auroral emission events and that of the directed sandpile models suggests that the turbulent magnetotail exhibits a significant degree of cross-scale energy transfer through localized dissipation events analogous to avalanches in SOC models. If one is to accept this suggestion, however, it is of critical importance to identify the primary physical process in the tail that could be responsible for such behavior.

1.2. Auroral Emission and Magnetotail Reconnection Dynamics

[9] *Uritsky et al.* [2002, 2003, 2006] and *Klimas et al.* [2000, 2004, 2005] have argued that the apparent SOC dynamics of the nighttime auroral emissions events is, in fact, a reflection of the SOC dynamics of the magnetotail reconnection system, where the actual critical state can be found. Their argument rests heavily on the observed relationship of fast flows and reconnection in the plasma sheet to consequent auroral illumination [*Ieda et al.*, 2001; *Zong et al.*, 2007], as mapped, one to the other, using one or more of the Tsyganenko magnetospheric magnetic field models [*Tsyganenko*, 1989, 1995, 1996, 2002; *Tsyganenko and Sitnov*, 2005]. As pointed out by *Liu et al.* [2006], however, reconnection in the tail occurs tailward of the inner region, where some of the auroral activity included in the studies of Uritsky et al. maps. Consequently, Liu et al. have constructed and studied the properties of a two-dimensional cellular automaton that models the dynamics of magnetic flux tubes in the region earthward of ~15 R_E.

[10] We feel that the argument of *Liu et al.* [2006] is somewhat overstated; when arguing against the reconnection explanation for the auroral emission statistics, they limit their attention to the region 20–30 R_E tailward of Earth, where reconnection is most prominent [*Nagai et al.*, 1998], while ignoring more earthward reconnection observations. Recently, *Sergeev et al.* [2007] have reported observations of strong repeated reconnection events earthward of ~14 R_E. They noted other observations and discussions of reconnection in that region [*McPherron and Manka*, 1985; *Sergeev et al.*, 1995; *Baker et al.*, 1996; *Miyashita et al.*, 2005; *Petrukovich and Yahnin*, 2006] and suggested that reconnection there may be more prevalent than is commonly assumed. Nevertheless, as we show here, Liu et al. are correct in pointing out that some of the auroral emission events included in the studies of *Uritsky et al.* [2002, 2003, 2006] do map to the inner magnetosphere, where reconnection has not been observed.

1.3. Latitudinal Dependence of Auroral Emission Event Dynamics

[11] In this study, we examine the mapping issue mentioned in section 1.2 to investigate its relevance to the conclusions of *Uritsky et al.* [2002, 2003, 2006] of inner and outer magnetotail activity. Previously, in our recent papers, as a proxy for mapping distance into the tail, the distribution with magnetic latitude (MLAT) of UVI auroral emission events (events, as defined in section 1.1) was divided into two separate groups of low-latitude (LL) and high-latitude (HL) events. The latitude of the onset of each event was used for the latitude of the event. *Uritsky et al.* [2008] noted that this distribution with latitude has a sharp peak at MLAT = 66°; all events originating below this latitude (down to 55°) were grouped as LL events and all events originating above it (up to 80°) were grouped as HL events. *Uritsky et al.* [2009] noted that the latitudes spanned by the auroral oval vary systematically with magnetic local time (MLT), so it is suboptimal to use only MLAT to separate higher- and lower-latitude events. Their idea was that since the oval latitude increases with longitudinal distance from midnight, simply using MLAT is not enough to guarantee that the

higher-latitude events are actually higher relative to an auroral boundary (such as the equatorward boundary of the oval). *Uritsky et al.* [2009] carried out this grouping in a manner more directly related to mapping distance in the tail. They used distance of an onset in MLAT relative to a realistic oval shape. For that shape, they used a function based on the empirical model of the ion isotropy boundary [*Gvozdevsky and Sergeev*, 1995; *Sergeev and Gvozdevsky*, 1995]. Both of these recent studies led to the conclusion that the HL group is characterized by nearly perfect power law statistics over the entire range of available scales, in agreement with the earlier studies of *Uritsky et al.* [2002, 2003, 2006], while the LL events constitute a scale-dependent statistical population with an energy crossover separating large and small auroral activations. Assuming the relationship of MLAT to distance into the tail, these results suggest an essentially scale-free energy release dynamics in the outer central plasma sheet (CPS) and a more complicated, scale-dependent dissipation in the inner CPS. *Uritsky et al.* [2009, p. 745] conjectured "that the inner and outer portions of the plasma sheet are associated with two (or more) mechanisms of collective dynamics that may represent an interplay between current disruption and magnetic reconnection scenarios of bursty energy conversion in the magnetotail."

1.4. Auroral Emission Events Mapped Into the Tail

[12] For the purpose of classifying the auroral emission events into two groups that may be related to activity in the inner versus the outer portions of the CPS, the use of the isotropic boundary model by *Uritsky et al.* [2009] was certainly an improvement over the more arbitrary division based on the peak in the MLAT distribution of the events. However, the isotropic boundary model can still be a poor representation of the actual boundary on a case-by-case basis, particularly during active times [*Donovan et al.*, 2003; *Meurant et al.*, 2007].

[13] In this paper, we improve the relationship of emission event position to possible activation source position by mapping the events into the tail using the Tsyganenko/Sitnov TS05 [*Tsyganenko and Sitnov*, 2005] and Tsyganenko T96 [*Tsyganenko*, 1995, 1996] magnetospheric field models. We rely on the ability of these models to respond to recent solar wind and geomagnetic activity to reconfigure the modeled magnetotail accordingly, in contrast to the static isotropic boundary model. The responses of these models to solar wind and geomagnetic activity can be expected to differ. The T96 model was constructed using essentially all near-Earth magnetometer data available at the time; the model is a best fit to data obtained during a variety of geomagnetic activity levels. Furthermore, the solar wind and geomagnetic activity, represented by *Dst*, enter the model as instantaneous parameters; the previous history of these parameters does not enter. In contrast, the TS05 model was constructed using a sophisticated evolution representation of the solar wind and geomagnetic activity inputs, including individual growth and relaxation forms, but its construction was based solely on storm time data. For our purposes, we can expect this model to provide better mapping during active times when the tail is stretched, times most pertinent to our study. However, while it is well known that storm intervals typically include several large substorms [*Wu et al.*, 2004], we do not expect either of these models to well represent the extremely stretched field configuration that may develop in the tail leading up to substorm onset. Nevertheless, *Uritsky et al.* [2009] have shown that the auroral emission events in this study can be classified into three groups: HL events that exhibit scale-free statistics and two LL groups, characterized by high and low emission energies. The LL, high-energy group constitutes approximately 0.3% of all of the events but almost 60% of the total auroral precipitation energy due to all of the events. These are almost certainly LL auroral substorm onsets associated with the extremely stretched tail field for which our mapping probably fails. Owing to their small number and localization to low latitudes, we assume that these events do not significantly affect our results. As we show in section 2.2, the results of this mapping study for the two Tsyganenko field models differ significantly beyond ~12 R_E down the tail but they are quite consistent up to 12 R_E, which is sufficient for our study. Given the fundamentally different bases of the two models, with one more sensitive to stretching than the other, this agreement can be considered evidence in support of our assumption that our results are not significantly affected by the possible failure of the Tsyganenko models during periods of extreme stretching.

[14] Our conclusions are based primarily on the TS05 model, using only events that map to within 15 R_E, where the model is expected to remain accurate, with the T96 event mapping included for corroboration, as explained above. We show that by mapping the *Uritsky et al.* [2002, 2003, 2006] auroral emission events into the magnetotail the tail can be divided into two regions, a region deeper in the tail where scale-free statistics indicative of a critical state are exhibited and a region more earthward where characteristic scales exist, with a transition between the two at approximately $|X_{\mathrm{GSM}}| = 12\ R_E$. We conclude that our statistical results are organized optimally by X_{GSM} and that the statistics are scale-free in the region beyond $|X_{\mathrm{GSM}}| \simeq 12\ R_E$, which is consistent with the region in the tail where reconnection has been observed [*McPherron and Manka*, 1985; *Sergeev et al.*, 1995, 2007; *Baker et al.*, 1996; *Miyashita et al.*, 2005; *Petrukovich and Yahnin*, 2006].

2. Mapping Analysis

[15] We have based our analysis on a collection of digital images of nighttime northern aurora (55–80 MLAT, 2000–0400 MLT) obtained from the UVI on board the Polar spacecraft, in the 165.5–174.5 nm portion of the Lyman-Birge-Hopfield spectral band, using an integration time of 36.5 s and a time resolution of 184 s. The studied database includes 16,000 images taken during two observation periods (1 January 1997 to 28 February 1997 and 1 January 1998 to 28 February 1998), both close to a solar minimum. The images were rebinned down to a uniform spatial resolution of 70 × 70 km^2, which was kept constant irrespective of the spacecraft altitude.

2.1. Identification of Auroral Events

[16] In contrast to statistical approaches dealing with individual auroral images such as the one described by *Lui et al.* [2000], our study involved spatiotemporal tracking of emission events as briefly explained below. In most cases,

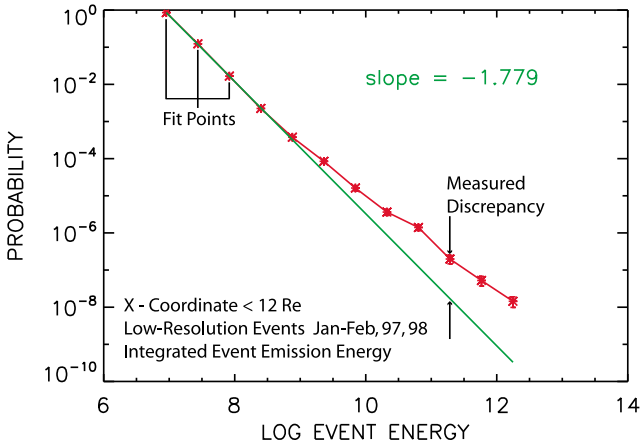

Figure 1. Probability distribution (red) of emission energy (arbitrary units) obtained for auroral precipitation events with TS05 mapped magnetotail positions within $|X_{GSM}| = 12\ R_E$. Power law fit (green) to first three small-energy distribution points as well as discrepancy between distribution and fit associated with large-energy crossover (see text) are shown.

this tracking made it possible to identify the precipitation events that coevolved in multiple auroral locations and could not be resolved otherwise [*Uritsky et al.*, 2002]. The UV luminosity was analyzed as a function of time and position on the image plane. First, active auroral regions were identified by applying the lower activity threshold representing a background UV flux. Adjacent spatial regions above the threshold were treated as parts of evolving events. By checking for overlap of common pixels between each pair of consecutive UVI frames, we identified a set of three-dimensional spatiotemporal domains corresponding to each of the individual emission events found by this method. Thus, the events were defined as connected regions in space-time. These domains of contiguous activity were used to evaluate the energy of each event given by the integral of the emission flux over the corresponding domain, as well as the spatiotemporal size of the event given by the volume of this domain (see *Uritsky et al.* [2008] for full definitions).

[17] To ensure sufficient accuracy in the determination of the ionospheric coordinates of the emission events, it was required that their initial area occupy no more than 10 pixels on a coarse-grained 70 × 70 km^2 grid. The largest initial area of the auroral events included in our analysis is therefore ~5 × 10^4 km^2, suggesting a linear dimension of about 200–300 km, depending on the configuration of the event. Given this filtering condition, the standard error in the calculation of the average central magnetic longitude and latitude of each emission event was about 35 km in the ionospheric frame.

[18] The initial central position of each auroral event was used as the input for the mapping procedure described below. For the plasma sheet region $|X_{GSM}| = 10$–$15\ R_E$, the main focus of our study (see below), the magnetospheric models used here result in an azimuthal mapping factor of 20–30. On the basis of our uncertainty of approximately 35 km at the ionosphere, the expected uncertainty in the determination of Y positions in the tail is ~1000 km or less. The radial mapping factor can vary significantly with geomagnetic activity level, leading to X errors of about 1 R_E for quiet to moderate magnetospheric activity and up to several Earth radii for a highly stretched magnetotail. Thus, we estimate that the accuracy of our conclusion concerning the position in the tail where the transition from scale-dependent to scale-free activity lies is limited by this uncertainty to no better than ~1 R_E. As discussed above, it appears that the highly stretched tail intervals do not contribute significantly to our results and so the error in our conclusion concerning the transition position in the tail is probably not much larger than this lower limit.

[19] The robustness of the auroral emission statistics with respect to changes in the activity threshold was verified earlier by repeatedly running the algorithm with substantially different threshold values [*Uritsky et al.*, 2002]. Here we show the results for the threshold of 10 photons cm^{-2} s^{-1} for consistency with our preceding publications dealing with the latitudinal dependence of statistical properties of the emission events.

2.2. Mapping Results

[20] We restrict our analysis to the auroral emission events collected by *Uritsky et al.* [2002] using the low-time-resolution UVI image data of January and February, 1997 and 1998. We select among these events on the basis of where they map into the tail using the two Tsyganenko models (T96 and TS05). Field lines are mapped into the tail from the positions at which the individual emission events originate and the corresponding positions in the tail are chosen by finding the maximum curvature along each field line (which has been found to correspond to the position on the field line at maximum radial distance). We use the maximum curvature as a proxy for the position of the cross-tail current sheet in the model.

[21] The red curve of Figure 1 shows the probability distribution of the *Uritsky et al.* [2002, 2003, 2006] low-time-resolution auroral emission events as a function of energy emitted over their lifetimes in arbitrary units (see the Uritsky et al. papers for information on the UV emission band and conversion to dimensional units) for the subset of events that have been found to map to $|X_{GSM}| < 12\ R_E$ using the TS05 field model. The distribution can be reasonably fit with two power law segments with a steeper slope for the low-energy events and a shallower slope for the high-energy events, showing the possibility of two collective modes of activity in the inner plasma sheet. Similar results have been obtained by *Uritsky et al.* [2008, 2009] for their LL events. *Uritsky et al.* [2008] have attributed their low-energy LL events mostly to diffuse auroral forms and have noted that their high-energy LL events may be due to substorm onset events. Reconnection is unlikely in this inner region ($|X_{GSM}| < 12\ R_E$) but current diversion [*Lui et al.*, 1991; *Lui*, 1996] may be contributing.

[22] Figure 1 also illustrates the method that we have used to quantify the discrepancy between relevant probability distributions and perfect power law forms. The green line in Figure 1 shows a least squares power law fit to the first three (lowest-energy) points of the distribution. For each of the points on the probability distribution, the discrepancy, on the log scale, between the distribution and the power law fit has been measured and an RMS measure of the overall discrepancy constructed. This method has been used to

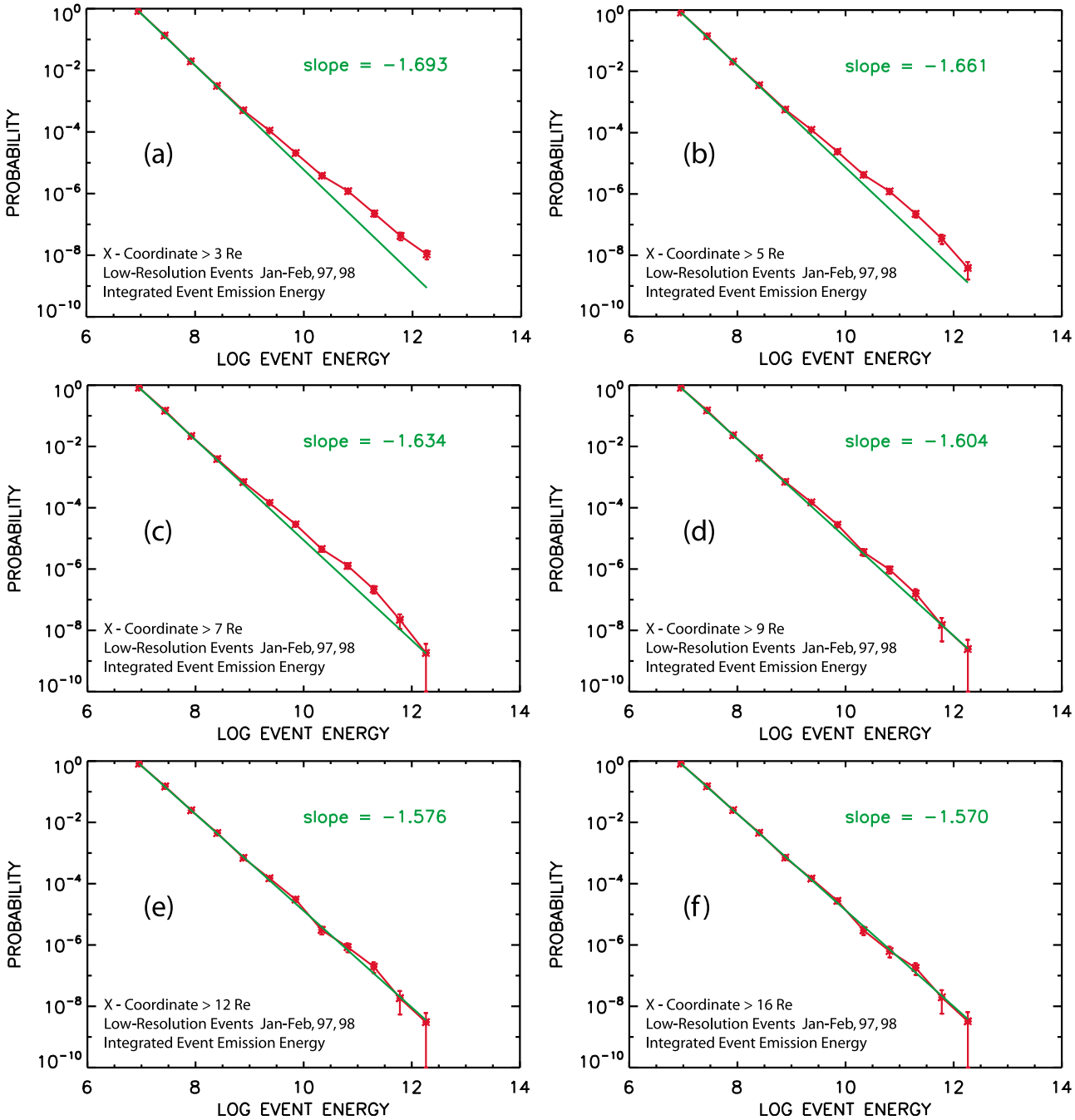

Figure 2. Energy distributions for all emission events whose TS05 mapped positions in the magnetotail are at $|X_{GSM}| >$ (a) 3 R_E, (b) 5 R_E, (c) 7 R_E, (d) 9 R_E, (e) 12 R_E, and (f) 16 R_E. Note the transition from scale-dependent (non-power law) to scale-free (power law) form as more near-Earth events are excluded.

obtain all of the results discussed below. All power law fits shown below are to only the first three points of the relevant probability distribution with an RMS measure of the discrepancy between the distribution and the power law fit computed accordingly.

[23] Figure 2 contains a sequence of emitted-energy probability distributions and their fits that has been constructed by including in the calculation of the distributions all emission events found to map, using TS05, to beyond a set of increasing $|X_{GSM}|$ values in the range from 3 to 16 R_E. It can be seen that, for a minimum cutoff $|X_{GSM}| = 3\ R_E$, the power law fit is steeper than for the rest of the examples shown due to the inclusion of most of the low-energy LL events discussed above in relation to Figure 1. The discrepancy between distribution and power law fit is at its largest for this low cutoff value because the high-energy LL events discussed by *Uritsky et al.* [2008] are included, leading to a shallower slope at high energies, similar to Figure 1. The slopes of the power law fits decrease monotonically with increasing cutoff while the contributions of the excess high-energy events gradually vanish. Overall, it is clear that the RMS discrepancy and the slopes of the

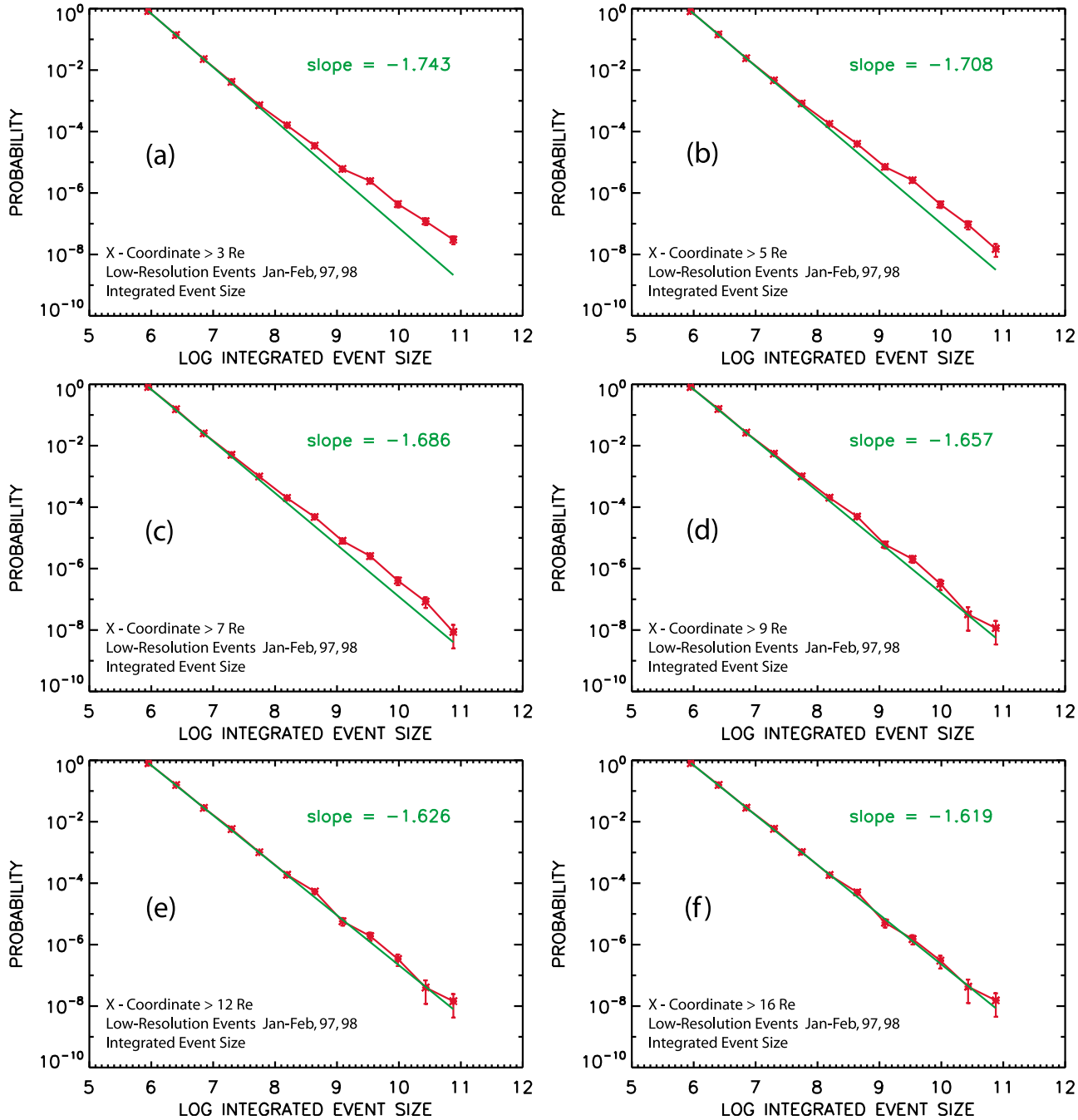

Figure 3. Integrated size distributions for all emission events whose TS05 mapped positions in the magnetotail are at $|X_{GSM}| >$ (a) 3 R_E, (b) 5 R_E, (c) 7 R_E, (d) 9 R_E, (e) 12 R_E, and (f) 16 R_E. Note the transition from scale-dependent (non-power law) to scale-free (power law) form as more near-Earth events are excluded.

power law fits decrease with increasing cutoff with very little change between 12 and 16 R_E.

[24] It is important to note that each of the distributions shown in Figure 2 is normalized to produce a probability. Thus, the number of events contained in any one distribution cannot be discerned from Figure 2. However, the significant change in the distributions shown, for example, in Figures 2a and 2b indicates that a significant number of events map to the interval $|X_{GSM}| = 3$–5 R_E, perhaps a surprisingly small tailward distance. A visual examination of many of these events has shown that many, and perhaps most or all, of these events map to reasonable radial distances but with large eastward or westward directions such that their projections to the $|X_{GSM}|$ direction are small.

[25] Figure 3 shows a sequence of probability distributions and their fits, similar to the sequence of Figure 2, but in this case for event size (emission region area, summed over the sequence of UVI images for which the event exists) rather than emitted energy; the minimum cutoff values are identical for both figures. The evolution of power law fit,

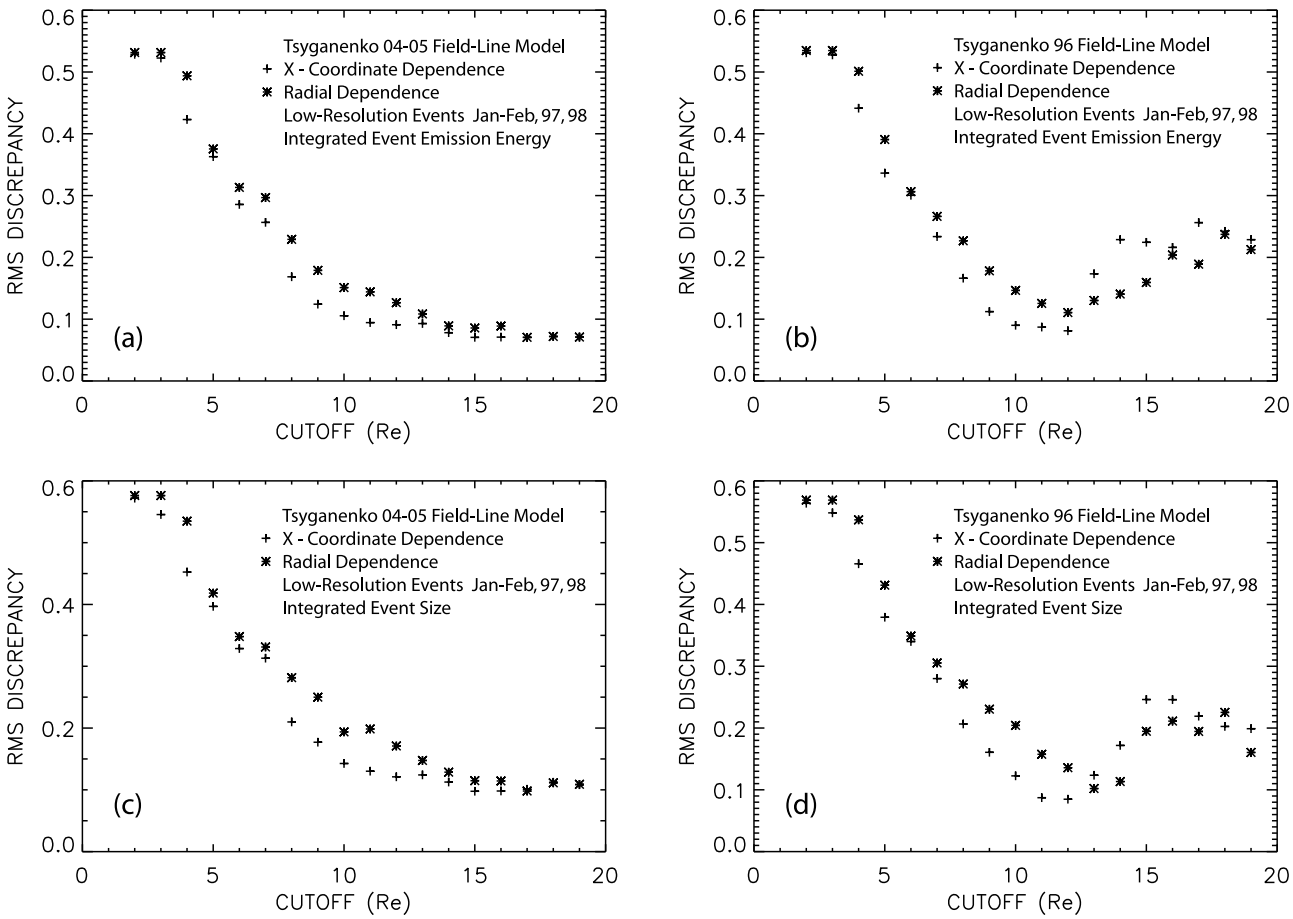

Figure 4. Showing the RMS difference between measured probability distributions and power law fits as explained in the text for (a) integrated event energy using the TS05 field line model for selection criteria, (b) integrated event energy using the T96 field line model for selection criteria, (c) integrated event size using the TS05 field line model for selection criteria, and (d) integrated event size using the T96 field line model. Each panel shows the results of using the maximum field line radius or the $|X_{GSM}|$ value at the position of that maximum for the mapped position of an event.

distribution shape, and discrepancy with increasing minimum cutoff is quite similar for both the energy and the size distributions. It should be noted that power law distributions over extended ranges for both energy and size distributions are considered significant evidence for SOC in distributed avalanching systems [*Bak et al.*, 1987, 1988]. We note that the slopes of the effectively scale-free distributions shown for $|X_{GSM}| = 12\ R_E$ or higher are close to, but slightly higher than, those given by *Uritsky et al.* [2002]. These differences are discussed in section 3.

[26] The evolution shown in Figures 2 and 3 implies the existence of a transition from non-scale-free to scale-free probability distributions that occurs as the field line mapped selection criterion is advanced from small to large distances in the tail, thereby removing an increasing number of inner magnetosphere associated emission events from consideration. We have examined this transition quantitatively in the selection range 3–19 R_E in 1 R_E increments by calculating the RMS discrepancy between the computed probability distribution values and the corresponding power law fits as explained above. We emphasize that the power law fits are to only the first three data points in the distributions (lowest energies or sizes). Figure 4 shows the results of this analysis for both emission event energy and integrated size probability distributions. Results obtained using both T96 and TS05 models are shown.

[27] All panels of Figure 4 indicate a clear transition from a poor to a good fit to a power law scale-free distribution as an increasing number of inner magnetosphere associated emission events are removed from consideration. The transitions found using the T96 and TS05 models are in good agreement out to $|X_{GSM}| \simeq 12\ R_E$, beyond which the T96 results become unreliable due to increasing noise on the distributions. Two selection criteria have been used to classify the emission events; both the maximum radius of the field line originating at the emission event and the $|X_{GSM}|$ value at the position of that maximum radius have been used. The more rapid decay of the curves based on $|X_{GSM}|$, plus the ultimate joining of the $|X_{GSM}|$- and radius-based curves, implies that the transition in the tail leading from non-scale-free to scale-free statistics is ordered by $|X_{GSM}|$, not the radius. We have not found comparable ordering with respect to other conceivable measures of position in the tail. The TS05 field model is expected to

remain accurate out to $|X_{GSM}| \simeq 15\ R_E$ (N. A. Tsyganenko, private communication, 2005). We take the first minimum inside of 15 R_E in the $|X_{GSM}|$-based curves as the position where the transition to scale-free statistics occurs. Our estimate is that the region in the tail leading to scale-free statistics in the auroral emission events is beyond approximately 12 R_E in $|X_{GSM}|$. For those events that map to the inside of 12 R_E, we find non-scale-free statistics.

3. Summary of Results

[28] We have reexamined the functional forms of the energy and size distributions of bright, nightside auroral emission events as observed by the UVI experiment on the Polar spacecraft and discussed previously by *Uritsky et al.* [2002, 2003, 2006, 2008, 2009]. We find that the events can be divided into two groups: (1) those that map to $|X_{GSM}| < 12\ R_E$ in the magnetotail and do not show scale-free statistics and (2) those that map to $|X_{GSM}| > 12\ R_E$ and do show scale-free statistics. We have found that the $|X_{GSM}|$ dependence most effectively organizes our events into these two groups.

[29] The power law distributions that we have obtained for group 2 are slightly steeper than those found by *Uritsky et al.* [2002] but they are nevertheless consistent with their results. The slight differences in slopes can be understood when account is taken of the fact that Uritsky et al. included all events in their analysis while we have removed group 1, which produces an excess in the distributions at high sizes or energies. The differences are too small to invalidate any of the conclusions that *Uritsky et al.* [2002, 2003, 2006] drew from their analyses concerning the existence of a critical state in the magnetosphere and its properties.

[30] Reconnection is most commonly observed in the 20–30 R_E range in the tail but it has been observed as close as 10–15 R_E [*McPherron and Manka*, 1985; *Sergeev et al.*, 1995; *Baker et al.*, 1996; *Miyashita et al.*, 2005; *Petrukovich and Yahnin*, 2006], where it has been suggested [*Sergeev et al.*, 2007] that due to observational difficulties reconnection may be more common than is indicated by the frequency of observations. We are unaware of any closer reconnection observations and so we take the 10–15 R_E range as an estimate of the inner boundary of the reconnection domain of the tail.

[31] The division at $|X_{GSM}| \simeq 12\ R_E$ between groups 1 and 2 of the auroral emission events coincides with the inner boundary of the reconnection domain of the tail. We interpret this coincidence as further support for our suggestion that the observed SOC dynamics of the auroral emission events is a reflection of a critical state in the magnetotail that is based on the dynamics of reconnection in the plasma sheet beyond $|X_{GSM}| = 12\ R_E$. It should be noted that the division at $\simeq 12\ R_E$ also coincides with the region of current diversion suggested as a substorm onset mechanism by *Lui et al.* [1991] and *Lui* [1996]. Furthermore, *Sergeev et al.* [2007] have observed signatures of current diversion coincident with their detection of strong reconnection in this region. They concluded that both reconnection and current diversion are essential elements of localized instability in this region of the tail and questioned whether one of these might be the driver of the other. For our present analysis, it is not important which of these two mechanisms drives the other, as long as reconnection takes part.

4. Final Remarks

[32] We feel that the interpretation of the observed SOC dynamics of the auroral emission events as a reflection of a critical state in the magnetotail that is based on the dynamics of reconnection in the plasma sheet remains a viable one. Other elements in our argument in support of this interpretation are summarized in the following.

[33] 1. The first of these is based on the scale-free nature of the observations with the largest energies, sizes, and lifetimes clearly due to substorms. The UVI images can be examined to see that many of the relatively few largest events are, indeed, substorms. At these scales, then, it is clear that the auroral emissions driver lies in the tail. It is difficult to imagine how a different driver at a different location could contribute to the smaller scales with statistical properties merging so smoothly with those of the larger scales and with no indication of characteristic scales. In fact, there is a considerable body of observational evidence that indicates that the smaller-scale auroral emission events are produced by a continuation of reconnection activity in the tail down to smaller events. Many studies have shown the close relationship between fast flows observed in the plasma sheet and auroral brightening in the ionosphere [*Sergeev et al.*, 1998; *Fairfield et al.*, 1999; *Lyons et al.*, 1999; *Zesta et al.*, 2000; *Ieda et al.*, 2001; *Nakamura et al.*, 2001a, 2001b]. The association of fast flows, plasmoid releases, and auroral emissions with substorm activity at the largest scales is well known. This association at the other extreme, localized reconnection as indicated by plasmoid observations during otherwise quiet intervals, has been clearly demonstrated in a recent paper by *Zong et al.* [2007] and earlier by *Ieda et al.* [2001]. Using GEOTAIL plasma sheet observations, Ieda et al. identified 24 plasmoid release events for which Polar UVI auroral image data were available. For all 24 of the events, associated auroral brightening was observed; there were no exceptions. The $|X_{GSM}| = 12\ R_E$ boundary separating the scale-free and scale-dependent tail dynamics according to our analysis is consistent with the region in the magnetotail where the fast tailward flows begin to decelerate. *Shiokawa et al.* [1997] have found that the high-speed flows are stopped at the boundary between the regions of dipolar field and taillike field in the plasma sheet. Our observations clearly show that the tailward region where the breaking mechanism should be much less efficient is also the source of scale-free auroral precipitation dynamics.

[34] 2. Cellular automata sandpile models are the prototypical SOC models. Remarkably, there are several suggestive analogies between the structure and behavior of these models and of the active magnetotail.

[35] In their most common form, sandpile models govern the transport of a conserved quantity, represented as grains, from a region that may be distributed or local where the grains are loaded to typically a boundary where the grains are unloaded. Transport in these models is enabled by the excitation of a threshold instability that is spatially localized; there are many of these instability sites distributed throughout the system. Under loading, these models evolve

(self-organize) into a state in which all of these sites are near the threshold for excitation. In this state, with continuing loading, long-ranged interactions between the sites of instability develop due to "avalanches" of the conserved quantity through the system. Avalanches of all sizes that can be contained within the system occur and the dynamics on different spatial scales is then self-similar. This self-similarity is manifested as power law relations between various characteristics of the particular model as well as through power law probabilities over spatial, temporal, and other scales.

[36] In the magnetotail, much of the transport of magnetic flux and energy through the tail is enabled by reconnection, which can be localized [see *Angelopoulos et al.*, 1999, and references therein]. The occurrence of active reconnection sites in the plasma sheet is correlated with recent loading, from which we can infer that a threshold for excitation of reconnection exists; that is, transport can be enabled by the excitation of a localized threshold instability. Fast flows, presumed to be generated by localized reconnection, can be observed in the plasma sheet at almost any time, although with varying probability. This observation shows that a spatially extended portion of the plasma sheet remains close, in varying degree, to the threshold of instability that leads to the transport-enabling localized reconnection. We can infer a critical state in which the entire relevant region of the plasma sheet is more or less near the threshold of instability, depending on the recent behavior of the solar wind. We should expect scale-free avalanche distributions of magnetic flux and energy through the system with sizes ranging from the basic element of instability, a single localized reconnection site, to a global scale, the substorm, with occurrence probability depending on the recent solar wind loading history. Our analysis presented in this paper supports this interpretation in that it shows that the observed scale-free auroral emissions dynamics is most closely associated with this region in the tail, where this scale-free avalanching should lie.

[37] 3. If the analogy detailed above is to hold, then reconnection must be localized always, even throughout the evolution of a substorm in the tail. *Lui et al.* [1998] have studied the association of reconnection activity in the tail with nightside UV auroral emissions and have found this requirement to be met. Using Polar UVI images containing auroral breakups and expansions, they identified a large number of substorm onsets during which GEOTAIL was in the plasma sheet. For each onset, they examined the plasma measurements at GEOTAIL over an interval stretching from 20 min before to 20 min after the onset. Synoptic patterns of plasma velocity, perpendicular velocity, and magnetic field changes were constructed. As expected, a clear pattern of dipolarization following the onsets was found. However, just a few fast flows and no global flow pattern were found. Lui et al. concluded that the fast flows associated with dipolarization must be localized and transient. We can infer the same properties for the reconnection sites throughout the evolution of a substorm.

[38] 4. If the dynamics of the magnetotail evolves in the neighborhood of a critical state in which an extended portion of the plasma sheet is close to unstable to the excitation of localized reconnection sites, and if recent loading has brought the tail close to this critical state, then it is clear that further loading and/or an externally imposed disturbance can induce a substorm. The concept of an avalanching critical state in the magnetotail *suggests* the possibility of both externally and internally triggered substorms.

[39] Thus, we suggest the existence of a self-organized critical state in the magnetotail based on avalanching of magnetic flux and energy through the tail. Of course, a proof of such a state does not yet exist; we need to develop a better understanding of the relationship between the current sheet and the auroral emission dynamics before this can be done. However, the conclusion of our analysis in this paper showing the concurrence of the regions of probable scale-free dynamics and reconnection in the tail adds to the evidence in favor of its existence. Given the novelty of this paradigm for substorm activity in the magnetotail, plus the continuing absence of an alternate explanation of the SOC statistics of the auroral emission events, further study of the possibility of this critical state remains necessary.

[40] **Acknowledgments.** We would like to acknowledge the essential contributions to many aspects of our results by D. Fairfield, A. Richmond, S. Boardsen, and N. Tsyganenko. For this research, one of us (A.J.K.) was supported by NASA grant NNX08AG73G and by the MMS IDS grant NCC5-494.

[41] Philippa Browning thanks Zoltan Voros and another reviewer for their assistance in evaluating this paper.

References

Angelopoulos, V., T. Mukai, and S. Kokubun (1999), Evidence for intermittency in Earth's plasma sheet and implications for self-organized criticality, *Phys. Plasmas*, *6*(11), 4161–4168, doi:10.1063/1.873681.

Bak, P., C. Tang, and K. Wiesenfeld (1987), Self-organized criticality: An explanation of 1/*f* noise, *Phys. Rev. Lett.*, *59*(4), 381–384, doi:10.1103/PhysRevLett.59.381.

Bak, P., C. Tang, and K. Wiesenfeld (1988), Self-organized criticality, *Phys. Rev. A*, *38*(1), 364–374, doi:10.1103/PhysRevA.38.364.

Baker, D. N., T. I. Pulkkinen, V. Angelopoulos, W. Baumjohann, and R. L. McPherron (1996), Neutral line model of substorms: Past results and present view, *J. Geophys. Res.*, *101*(A6), 12,975–13,010, doi:10.1029/95JA03753.

Baker, D. N., T. I. Pulkkinen, J. Buchner, and A. J. Klimas (1999), Substorms: A global instability of the magnetosphere-ionosphere system, *J. Geophys. Res.*, *104*(A7), 14,601–14,611, doi:10.1029/1999JA900162.

Borovsky, J. E., and H. O. Funsten (2003), MHD turbulence in the Earth's plasma sheet: Dynamics, dissipation, and driving, *J. Geophys. Res.*, *108*(A7), 1284, doi:10.1029/2002JA009625.

Borovsky, J. E., R. C. Elphic, H. O. Funsten, and M. F. Thomsen (1997), The Earth's plasma sheet as a laboratory for flow turbulence in high-beta MHD, *J. Plasma Phys.*, *57*, 1–34, doi:10.1017/S0022377896005259.

Chang, T. (1992), Low-dimensional behavior and symmetry-breaking of stochastic systems near criticality—Can these effects be observed in space and in the laboratory? *IEEE Trans. Plasma Sci.*, *20*(6), 691–694, doi:10.1109/27.199515.

Chang, T. (1998a), Multiscale intermittent turbulence in the magnetotail, in *Substorms-4*, edited by S. Kokubun and Y. Kamide, pp. 431–436, Terra Sci., Tokyo.

Chang, T. (1998b), Sporadic localized reconnections and intermittent turbulence in the magnetotail, in *Geospace Mass and Energy Flow*, edited by J. L. Horwitz et al., pp. 193–199, AGU, Washington, D. C.

Chang, T. (1999), Self-organized criticality, multi-fractal spectra, sporadic localized reconnections and intermittent turbulence in the magnetotail, *Phys. Plasmas*, *6*(11), 4137–4145, doi:10.1063/1.873678.

Chang, T., and C. Wu (2002), "Complexity" and anomalous transport in space plasmas, *Phys. Plasmas*, *9*(9), 3679–3684, doi:10.1063/1.1499115.

Chang, T., S. W. Y. Tam, C. C. Wu, and G. Consolini (2003), Complexity, forced and/or self-organized criticality, and topological phase transitions in space plasmas, *Space Sci. Rev. 107*(1–2), 425–445, doi:10.1023/A:1025502023494.

Chang, T., S. W. Y. Tam, and C. C. Wu (2004), Complexity induced anisotropic bimodal intermittent turbulence in space plasmas, *Phys. Plasmas*, *11*, 1287–1299, doi:10.1063/1.1667496.

Consolini, G. (1997), Intermittency and turbulence in magnetospheric dynamics, in *Proceedings of the International School of Physics* "*Enrico Feremi*", IOS Press, Amsterdam.

Consolini, G., and T. S. Chang (2001), Magnetic field topology and criticality in geotail dynamics: Relevance to substorm phenomena, *Space Sci. Rev.*, *95*(1–2), 309–321, doi:10.1023/A:1005252807049.

Consolini, G., and T. Chang (2002), Complexity, magnetic field topology, criticality, and metastability in magnetotail dynamics, *J. Atmos. Sol. Terr. Phys.*, *64*(5–6), 541–549, doi:10.1016/S1364-6826(02)00011-1.

Donovan, E. F., B. J. Jackel, I. Voronkov, T. Sotirelis, F. Creutzberg, and N. A. Nicholson (2003), Ground-based optical determination of the b2i boundary: A basis for an optical MT-index, *J. Geophys. Res.*, *108* (A3), 1115, doi:10.1029/2001JA009198.

Fairfield, D. H., et al. (1999), Earthward flow bursts in the inner magnetotail and their relation to auroral brightenings, AKR intensifications, geosynchronous particle injections and magnetic activity, *J. Geophys. Res.*, *104*(A1), 355–370, doi:10.1029/98JA02661.

Gvozdevsky, B. B., and V. A. Sergeev (1995), MT-index—A possible new index to characterize the configuration of the magnetotail, *Adv. Space Res.*, *18*(8), 51–54, doi:10.1016/0273-1177(95)00995-7.

Hughes, D., and M. Paczuski (2002), Large scale structures, symmetry, and universality in sandpiles, *Phys. Rev. Lett.*, *88*(5), 054302, doi:10.1103/PhysRevLett.88.054302.

Ieda, A., D. H. Fairfield, T. Mukai, Y. Saito, S. Kokubun, K. Liou, C.-I. Meng, G. K. Parks, and M. J. Brittnacher (2001), Plasmoid ejection and auroral brightenings, *J. Geophys. Res.*, *106*(A3), 3845–3857, doi:10.1029/1999JA000451.

Jensen, H. J. (1998), Self-Organized Criticality: Emergent Complex Behaviour in Physical and Biological Systems, Cambridge Univ. Press, Cambridge, U. K.

Klimas, A. J., J. A. Valdivia, D. Vassiliadis, D. N. Baker, M. Hesse, and J. Takalo (2000), Self-organized criticality in the substorm phenomenon and its relation to localized reconnection in the magnetospheric plasma sheet, *J. Geophys. Res.*, *105*(A8), 18,765–18,780, doi:10.1029/1999JA000319.

Klimas, A. J., V. M. Uritsky, D. Vassiliadis, and D. N. Baker (2004), Reconnection and scale-free avalanching in a driven current-sheet model, *J. Geophys. Res.*, *109*(A2), A02218, doi:10.1029/2003JA010036.

Klimas, A. J., V. Uritsky, D. Vassiliadis, and D. Baker (2005), Simulation study of SOC dynamics in driven current-sheet models, in *Nonequilibrium Phenomena in Plasmas*, edited by A. S. Sharma and P. K. Kaw, pp. 71–89, Springer, Dordrecht, Netherlands.

Liu, W. W., P. Charbonneau, K. Thibault, and L. Morales (2006), Energy avalanches in the central plasma sheet, *Geophys. Res. Lett.*, *33*, L19106, doi:10.1029/2006GL027282.

Lu, E. T. (1995), Avalanches in continuum driven dissipative systems, *Phys. Rev. Lett.*, *74*(13), 2511–2514, doi:10.1103/PhysRevLett.74.2511.

Lui, A. T. Y. (1996), Current disruption in the Earth's magnetosphere: Observations and models, *J. Geophys. Res.*, *101*(A6), 13,067–13,088, doi:10.1029/96JA00079.

Lui, A. T. Y. (2001), Multifractal and intermittent nature of substorm-associated magnetic turbulence in the magnetotail, *J. Atmos. Sol. Terr. Phys.*, *63*(13), 1379–1385, doi:10.1016/S1364-6826(00)00239-X.

Lui, A. T. Y. (2002), Multiscale phenomena in the near-Earth magnetosphere, *J. Atmos. Sol. Terr. Phys.*, *64*(2), 125–143, doi:10.1016/S1364-6826(01)00079-7.

Lui, A. T. Y., C.-L. Chang, A. Mankofsky, H.-K. Wong, and D. Winske (1991), A cross-field current instability for substorm expansions, *J. Geophys. Res.*, *96*(A7), 11,389–11,401, doi:10.1029/91JA00892.

Lui, A. T. Y., K. Liou, P. T. Newell, C. I. Meng, S. I. Ohtani, T. Ogino, S. Kokubun, M. J. Brittnacher, and G. K. Parks (1998), Plasma and magnetic flux transport associated with auroral breakups, *Geophys. Res. Lett.*, *25*(21), 4059–4062, doi:10.1029/1998GL900022.

Lui, A. T. Y., S. C. Chapman, K. Liou, P. T. Newell, C. I. Meng, M. Brittnacher, and G. D. Parks (2000), Is the dynamic magnetosphere an avalanching system? *Geophys. Res. Lett.*, *27*(7), 911–914, doi:10.1029/1999GL010752.

Lyons, L. R., T. Nagai, G. T. Blanchard, J. C. Samson, T. Yamamoto, T. Mukai, A. Nishida, and S. Kokubun (1999), Association between Geotail plasma flows and auroral poleward boundary intensifications observed by CANOPUS photometers, *J. Geophys. Res.*, *104*(A3), 4485–4500, doi:10.1029/1998JA900140.

McPherron, R. L., and R. H. Manka (1985), Dynamics of the 1054 UT March 22, 1979, Substorm Event: CDAW 6, *J. Geophys. Res.*, *90*(A2), 1175–1190, doi:10.1029/JA090iA02p01175.

Meurant, M., J. C. Gerard, C. Blockx, E. Spanswick, E. F. Donovan, B. Hubert, V. Coumans, and M. Connors (2007), EL: a possible indicator to monitor the magnetic field stretching at global scale during substorm expansive phase: Statistical study, *J. Geophys. Res.*, *112*(A5), A05222, doi:10.1029/2006JA012126.

Miyashita, Y., et al. (2005), Plasmoids observed in the near-Earth magnetotail at $X \sim -7\ R_E$, *J. Geophys. Res.*, *110*, A12214, doi:10.1029/2005JA011263.

Munoz, M. A., R. Dickman, A. Vespignani, and S. Zapperi (1999), Avalanche and spreading exponents in systems with absorbing states, *Phys. Rev. E*, *59*(5), 6175–6179, doi:10.1103/PhysRevE.59.6175.

Nagai, T., et al. (1998), Structure and dynamics of magnetic reconnection for substorm onsets with Geotail observations, *J. Geophys. Res.*, *103* (A3), 4419–4440, doi:10.1029/97JA02190.

Nakamura, R., W. Baumjohann, M. Brittnacher, V. A. Sergeev, M. Kubyshkina, T. Mukai, and K. Liou (2001a), Flow bursts and auroral activations: Onset timing and foot point location, *J. Geophys. Res.*, *106*(A6), 10,777–10,789, doi:10.1029/2000JA000249.

Nakamura, R., W. Baumjohann, R. Schodel, M. Brittnacher, V. A. Sergeev, M. Kubyshkina, T. Mukai, and K. Liou (2001b), Earthward flow bursts, auroral streamers, and small expansions, *J. Geophys. Res.*, *106*(A6), 10,791–10,802, doi:10.1029/2000JA000306.

Paczuski, M., S. Maslov, and P. Bak (1996), Avalanche dynamics in evolution, growth, and depinning models, *Phys. Rev. E*, *53*(1), 414–443, doi:10.1103/PhysRevE.53.414.

Petrukovich, A. A., and A. G. Yahnin (2006), The substorm onset location controversy, *Space Sci. Rev.*, *122*(1–4), 81–87, doi:10.1007/s11214-006-7022-8.

Sergeev, V. A., and B. B. Gvozdevsky (1995), MT-index—A possible new index to characterize the magnetic configuration of magnetotail, *Ann. Geophys.*, *13*(10), 1093–1103.

Sergeev, V. A., V. Angelopoulos, D. G. Mitchell, and C. T. Russell (1995), In situ observations of magnetotail reconnection prior to the onset of a small substorm, *J. Geophys. Res.*, *100*(A10), 19,121–19,133, doi:10.1029/95JA01471.

Sergeev, V. A., M. A. Shukhtina, R. Rasinkangas, A. Korth, G. D. Reeves, H. J. Singer, M. F. Thomsen, and L. I. Vagina (1998), Event study of deep energetic particle injections during substorm, *J. Geophys. Res.*, *103*(A5), 9217–9234, doi:10.1029/97JA03686.

Sergeev, V., et al. (2007), Observation of repeated intense near-Earth reconnection on closed field lines with Cluster, Double Star, and other spacecraft, *Geophys. Res. Lett.*, *34*(2), L02103, doi:10.1029/2006GL028452.

Shiokawa, K., W. Baumjohann, and G. Haerendel (1997), Braking of high-speed flows in the near-Earth tail, *Geophys. Res. Lett.*, *24*(10), 1179–1182, doi:10.1029/97GL01062.

Tsyganenko, N. A. (1989), A magnetospheric magnetic-field model with a warped tail current sheet, *Planet. Space Sci.*, *37*(1), 5–20, doi:10.1016/0032-0633(89)90066-4.

Tsyganenko, N. A. (1995), Modeling the Earth's magnetospheric magnetic field confined within a realistic magnetopause, *J. Geophys. Res.*, *100*(A4), 5599–5612, doi:10.1029/94JA03193.

Tsyganenko, N. A. (1996), Effects of the solar wind conditions on the global magnetospheric configuration as deduced from data-based field models, in *Proceedings of the Third International Conference on Substorms (ICS-3)*, *Spec. Publ. ESA SP-389*, pp. 181–185, Eur. Space Agency, Noordwijk, Netherlands.

Tsyganenko, N. A. (2002), A model of the near magnetosphere with a dawn-dusk asymmetry: 2. Parameterization and fitting to observations, *J. Geophys. Res.*, *107*(A8), 1176, doi:10.1029/2001JA000220.

Tsyganenko, N. A., and M. I. Sitnov (2005), Modeling the dynamics of the inner magnetosphere during strong geomagnetic storms, *J. Geophys. Res.*, *110*, A03208, doi:10.1029/2004JA010798.

Uritsky, V., and A. Klimas (2004), Scaling and predictability of complex geospace disturbances, paper presented at the 7th International Conference on Substorms, Finn. Meteorol. Inst., Helsinki.

Uritsky, V. M., and M. I. Pudovkin (1998), Low frequency 1/*f*-like fluctuations of the AE-index as a possible manifestation of self-organized criticality in the magnetosphere, *Ann. Geophys.*, *16*(12), 1580–1588, doi:10.1007/s00585-998-1580-x.

Uritsky, V. M., A. J. Klimas, D. Vassiliadis, D. Chua, and G. D. Parks (2002), Scale-free statistics of spatiotemporal auroral emissions as depicted by POLAR UVI images: The dynamic magnetosphere is an avalanching system, *J. Geophys. Res.*, *107*(A12), 1426, doi:10.1029/2001JA000281.

Uritsky, V. M., A. J. Klimas, and D. Vassiliadis (2003), Evaluation of spreading critical exponents from the spatiotemporal evolution of emission regions in the nighttime aurora, *Geophys. Res. Lett.*, *30*(15), 1813, doi:10.1029/2002GL016556.

Uritsky, V., A. Klimas, and D. Vassiliadis (2006), Critical finite-size scaling of energy and lifetime probability distributions of auroral emissions, *Geophys. Res. Lett.*, *33*, L08102, doi:10.1029/2005GL025330.

Uritsky, V. M., E. Donovan, A. J. Klimas, and E. Spanswick (2008), Scale-free and scale-dependent modes of energy release dynamics in the nighttime magnetosphere, *Geophys. Res. Lett.*, *35*, L21101, doi:10.1029/2008GL035625.

Uritsky, V. M., E. Donovan, A. J. Klimas, and E. Spanswick (2009), Collective dynamics of bursty particle precipitation initiating in the inner and outer plasma sheet, *Ann. Geophys.*, *27*, 745–753.

Volwerk, M., et al. (2004), Multi-scale analysis of turbulence in the Earth's current sheet, *Ann. Geophys.*, *22*(7), 2525–2533.

Vörös, Z., et al. (2003), Multi-scale magnetic field intermittence in the plasma sheet, *Ann. Geophys.*, *21*(9), 1955–1964.

Vörös, Z., W. Baumjohann, R. Nakamura, A. Runov, M. Volwerk, T. L. Zhang, and A. Balogh (2004a), Wavelet analysis of magnetic turbulence in the Earth's plasma sheet, *Phys. Plasmas*, *11*(4), 1333–1338, doi:10.1063/1.1667499.

Vörös, Z., et al. (2004b), Magnetic turbulence in the plasma sheet, *J. Geophys. Res.*, *109*, A11215, doi:10.1029/2004JA010404.

Vörös, Z., W. Baumjohann, R. Nakamura, A. Runov, M. Volwerk, H. K. Schwarzl, A. Balogh, and H. Rème (2005), Dissipation scales in the Earth's plasma sheet estimated from Cluster measurements, *Nonlinear Process. Geophys.*, *12*(5), 725–732.

Vörös, Z., W. Baumjohann, R. Nakamura, M. Volwerk, and A. Runov (2006), Bursty bulk flow driven turbulence in the Earth's plasma sheet, *Space Sci. Rev.*, *122*(1–4), 301–311, doi:10.1007/s11214-006-6987-7.

Vörös, Z., W. Baumjohann, R. Nakamura, A. Runov, M. Volwerk, T. Takada, E. A. Lucek, and H. Reme (2007), Spatial structure of plasma flow associated turbulence in the Earth's plasma sheet, *Ann. Geophys.*, *25* (1), 13–17.

Weygand, J. M., M. G. Kivelson, K. K. Khurana, R. L. McPherron, L. M. Kistler, A. Balogh, and S. Thompson (2003), Probability distribution functions for magnetic field fluctuations inferred from Cluster measurements: Evidence for intermittent turbulence in the plasma sheet, *Eos. Trans. AGU*, *84*(46), Fall Meet. Suppl., Abstract SM32C-02.

Weygand, J. M., et al. (2005), Plasma sheet turbulence observed by Cluster II, *J. Geophys. Res.*, *110*, A01205, doi:10.1029/2004JA010581.

Weygand, J. M., M. G. Kivelson, K. K. Khurana, H. K. Schwarzl, R. J. Walker, A. Balogh, L. M. Kistler, and M. L. Goldstein (2006), Non-self-similar scaling of plasma sheet and solar wind probability distribution functions of magnetic field fluctuations, *J. Geophys. Res.*, *111*, A11209, doi:10.1029/2006JA011820.

Wu, C. C., and T. Chang (2000a), 2D MHD simulation of the emergence and merging of coherent structures, *Geophys. Res. Lett.*, *27*(6), 863–866, doi:10.1029/1999GL003704.

Wu, C. C., and T. Chang (2000b), Dynamical evolution of coherent structures in intermittent two-dimensional MHD turbulence, *IEEE Trans. Plasma Sci.*, *28*(6), 1938–1943, doi:10.1109/27.902222.

Wu, C. C., and T. Chang (2001), Further study of the dynamics of two-dimensional MHD coherent structures—A large-scale simulation, *J. Atmos. Sol. Terr. Phys.*, *63*(13), 1447–1453, doi:10.1016/S1364-6826(00)00246-7.

Wu, C.-C., K. Liou, R. P. Lepping, and C.-I. Meng (2004), Identification of substorms within storms, *J. Atmos. Sol. Terr. Phys.*, *66*, 125–132, doi:10.1016/j.jastp.2003.09.012.

Zesta, E., L. R. Lyons, and E. Donovan (2000), The auroral signature of Earthward flow bursts observed in the magnetotail, *Geophys. Res. Lett.*, *27*(20), 3241–3244, doi:10.1029/2000GL000027.

Zong, Q.-G., et al. (2007), Earthward flowing plasmoid: Structure and its related ionospheric signature, *J. Geophys. Res.*, *112*, A07203, doi:10.1029/2006JA012112.

E. Donovan and V. Uritsky, Department of Physics and Astronomy, University of Calgary, Calgary, AB T2N 1N4, Canada.

A. Klimas, NASA Goddard Space Flight Center, Greenbelt, MD 20771, USA. (alex.klimas@nasa.gov)